TURBULENCE, TRANSFER, AND EXCHANGE

BY JAMES N. MOUM,
JONATHAN D. NASH,
AND JODY M. KLYMAK

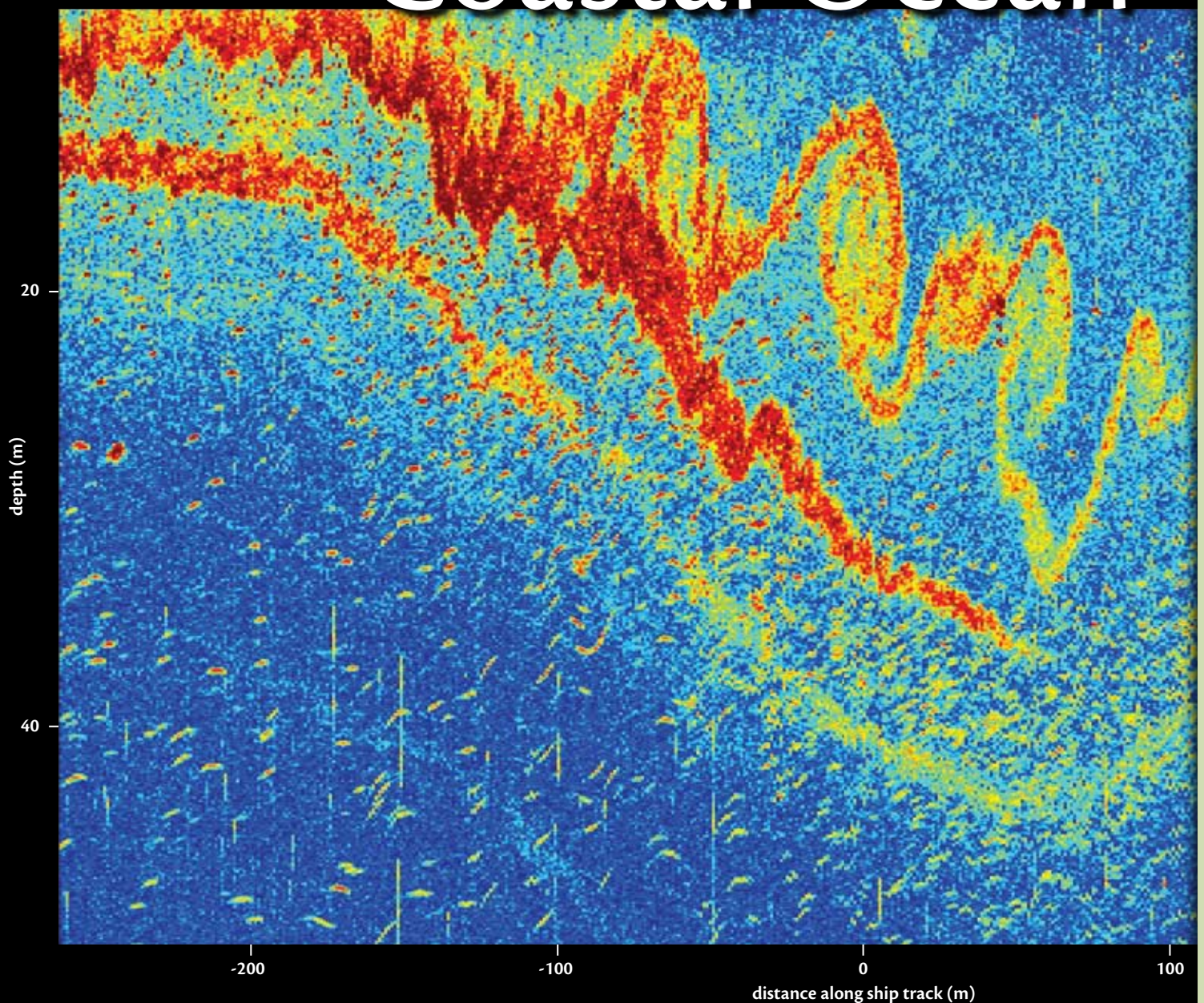# Small-Scale Processes
in the Coastal Ocean

ABSTRACT. Varied observations over Oregon's continental shelf illustrate the beauty and complexity of geophysical flows in coastal waters. Rapid, creative, and sometimes fortuitous sampling from ships and moorings has allowed detailed looks at boundary layer processes, internal waves (some extremely nonlinear), and coastal currents, including how they interact. These processes drive turbulence and mixing in shallow coastal waters and encourage rapid biological responses, yet are poorly understood and parameterized. The work presented here represents examples of efforts by many physical oceanographers to quantify small-scale, coastal-mixing processes so that their effects might be included in regional circulation models.
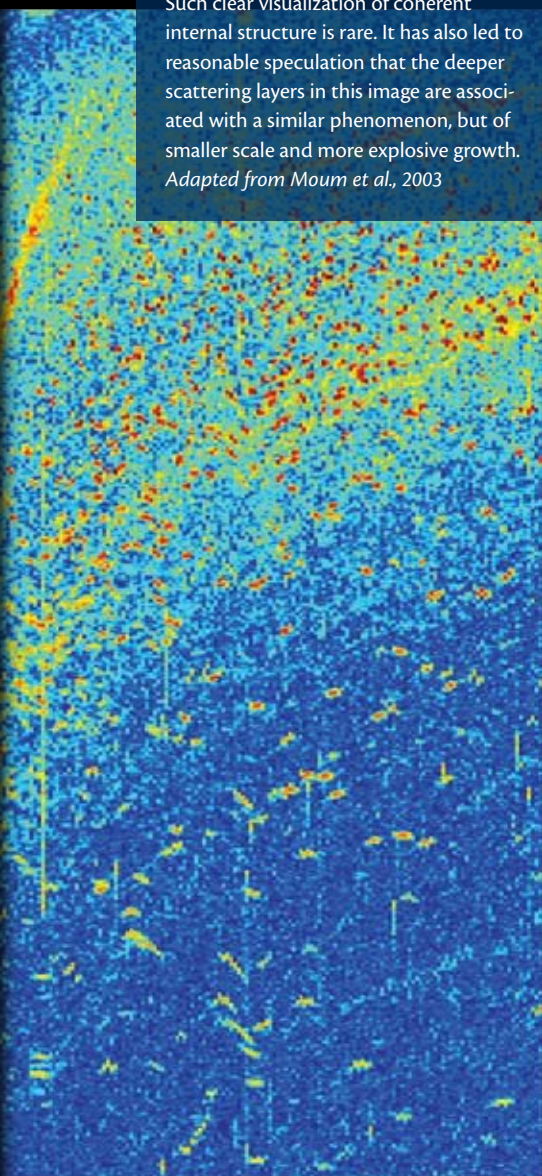
Figure 1. Kelvin-Helmholtz billows recently generated in a 30-m amplitude nonlinear internal wave propagating from left to right. The bright scattering layers trailing the wave trough are likely due to sound-speed microstructure. Such clear visualization of coherent internal structure is rare. It has also led to reasonable speculation that the deeper scattering layers in this image are associated with a similar phenomenon, but of smaller scale and more explosive growth. *Adapted from Moum et al., 2003*

200

INTRODUCTION

Coastal oceans have a wide range of fascinating and complex fluid motions that can only be captured by detailed sampling. The fluid dynamics represented can

- be beautiful to behold, as depicted in Figure 1, which shows growing Kelvin-Helmholtz billows within a propagating internal solitary wave— an example of waves within waves;
- excite rapid biological responses;
- create irreversible transports of mass, biomass, and nutrients and momentum that are difficult to parameterize in coastal circulation models.

Because of the multiplicity of small-scale processes and their complex nature, the prospects for sorting out their contributions to the larger-scale coastal circulation has seemed daunting. However, over the past decade, significant progress has been made in understanding fine-scale and turbulence dynamics over continental shelves. Targeted efforts using modern, rapid-sampling shipboard and bottom-mounted instrumentation have provided detailed observations leading

to a better appreciation for the role of small-scale processes in the coastal ocean. Such efforts have allowed for quantitative assessment of turbulence-closure models for some specific cases, such as the tidally mixed Celtic Sea (i.e., Simpson et al., 1996) and bottom boundary-layer turbulence on the Oregon shelf (i.e., Kurapov et al., 2005b), and they have offered the potential for improved turbulence parameterizations (i.e., MacKinnon and Gregg, 2003a). Here, we provide examples from our work over Oregon's continental shelf.

NEW PERSPECTIVES ON CROSS-SHELF STRUCTURE

It is difficult to obtain a satisfying measure of the detailed structure of coastal flows because

- the structure is three dimensional;
- the scales are O(10 km) in the cross-shelf dimension and larger in the alongshore dimension;
- they evolve on a range of time scales, including that of changes in the surface wind field, and from both observational and dynamical perspectives, on tidal and near-inertial time scales.

To obtain detailed observations of cross-shelf structure, perhaps the best we can do is to sample a fixed line across the shelf as rapidly as possible and consider the hypothesis that the flow is two dimensional. A sequence of cross-shelf transects at 11–20-h intervals were made with this in mind in late spring 2001 (during the CoOP-sponsored COAST program). Density/turbulence profiles were made directly from near the surface to the seafloor (within 2 cm of the bottom), allowing a detailed look at the structure and evolution of not only the coastal jet but also the bottom Ekman layer (Figure 2).

BOTTOM EKMAN LAYER

Although several important aspects of the coastal jet and the Ekman layer appear in Figure 2, we focus first on the fluid in the bottom boundary layer and interpret its motion in terms of basic Ekman dynamics, which dictates that the cross-shelf movement is determined
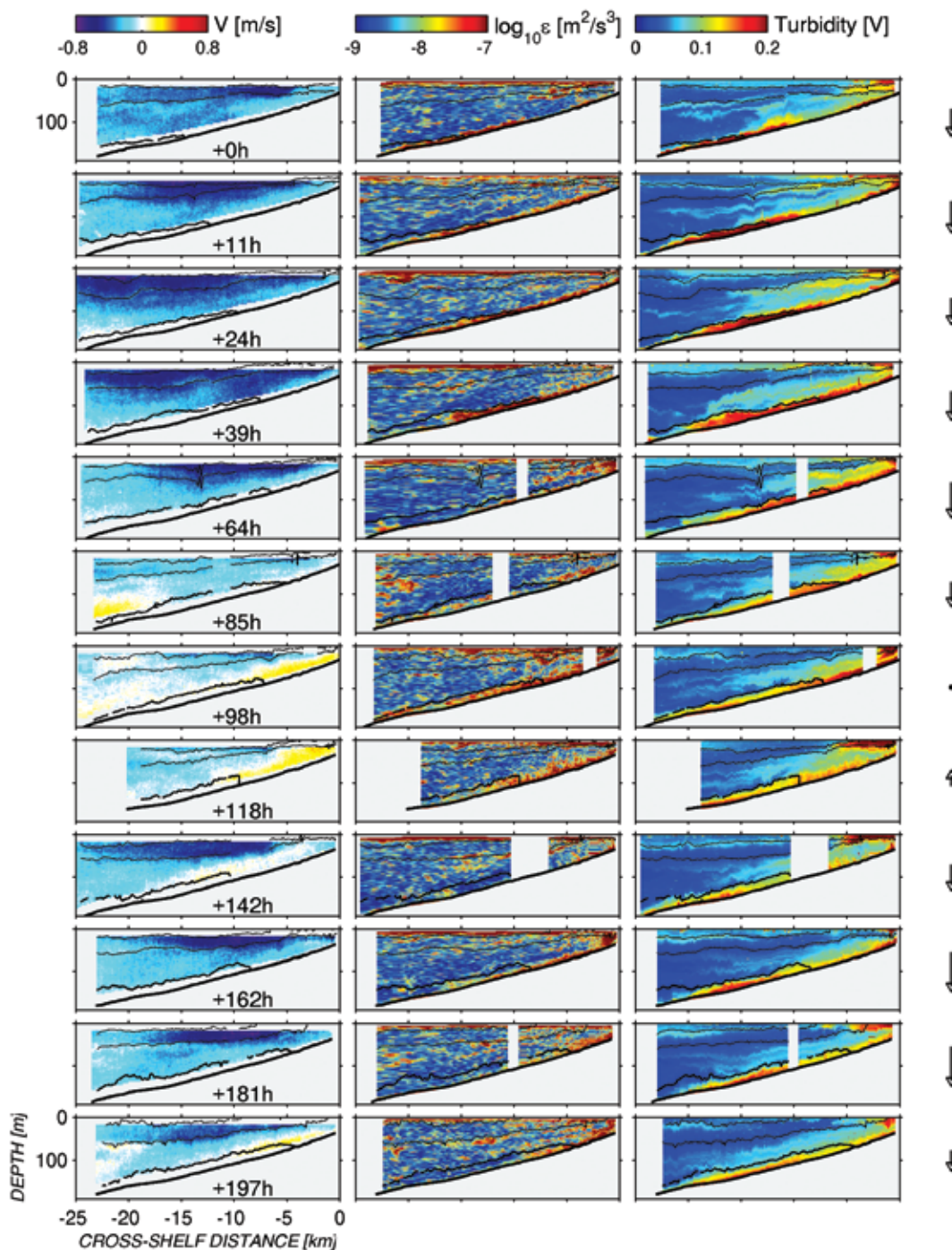

Figure 2. Evolution of the flow on the shelf showing coastal upwelling, its relaxation, and resumption. Summary of alongshore currents (V, lefthand column), turbulent dissipation rate (ε, middle column) and turbidity (880-nm optical backscatter measurements, right column) from an eight-day period in May/June 2001 during which 12 transects were made across the Oregon shelf off Cascade Head. Isopycnals are plotted over each image, the deepest isopycnal highlighted as an indicator of cross-shelf motion of the bottom boundary layer. Relative wind stress averaged over the 24-h period preceding each transect is shown to the right (upwelling-favorable down). The relative time of each transect is shown in the leftmost column, starting with 0 h at the beginning of the first transect. *Adapted from Perlin et al., 2005a*

solely by the bottom stress in the along-shelf direction (north-south off Oregon). The densest fluid is outlined by the deepest of the three isopycnals shown in Figure 2. As the wind (and current) remains steady and southward in the first 80 h, this fluid moves up the slope at speeds of several kilometers per day (1 km d$^{-1} \cong 1$ cm s^{-1}). As the wind relaxes and turns to the north, the current also reverses, and the densest fluid flows back down the slope, returning up the slope with resumption of southward winds (and southward currents). Predicting the Ekman transport requires an estimate of the bottom stress. At this location, a typical law-of-the-wall parameterization did not yield bottom stresses in agreement with either the observed Ekman transports or turbulence measurements of bottom stress (Perlin et al., 2005b). This situation has led to a modified bottom stress parameterization that accounts for the suppression of turbulence by stratification (Perlin et al., 2005a).

An important wrinkle in this straightforward interpretation occurs as upwelling relaxes (+98 h, +118 h). Individual vertical profiles indicate relatively light parcels of fluid near the seafloor at midshelf, producing a statically unstable state (Figure 3; Moum et al., 2004).
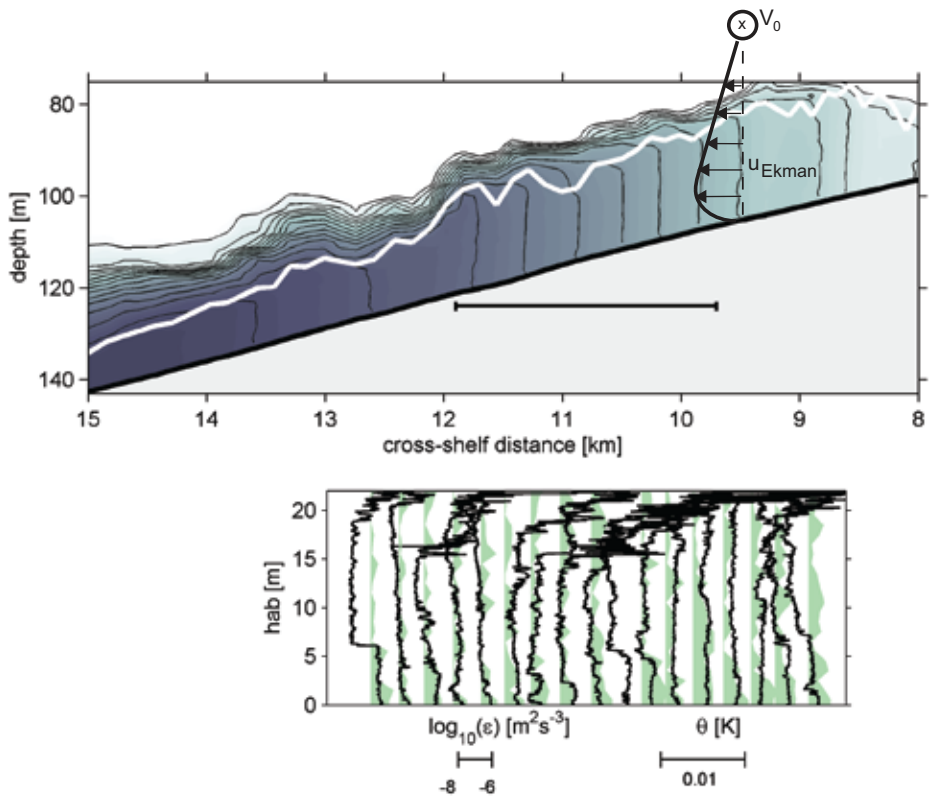

Figure 3. Convectively driven mixing in the bottom boundary (from data at +118 h in Figure 2). Density is color-imaged in the upper panel (darker is heavier fluid). Isopycnals are shown in black and the height of the bottom mixed layer in white. The upwelling-induced cross-shelf circulation has drawn dense fluid up the shelf. Upon relaxation and reversal of the winds (+98 h, +118 h), the near-bottom alongshore flow (V_0) reverses, inducing a cross-shore Ekman velocity profile similar to that shown, in which the bottom velocity must equal 0. This velocity profile combined with the induced cross-shore density gradient causes light fluid to be advected offshore beneath denser fluid above. The result is convectively driven mixing, depicted in the bottom panel, which shows vertical profiles of potential temperature (θ) and ε (shading) as functions of height above bottom (hab); the ordinate label, hab, refers to height above bottom. Numerous instantaneous examples of warm (light) fluid beneath cool (heavy) fluid can be seen. This instability acts to drive the near-bottom turbulence and thicken the bottom Ekman layer. *Adapted from Moum et al., 2004*

James N. Moum (*moum@coas. oregonstate.edu*) *is Professor, College of Oceanic and Atmospheric Sciences, Oregon State University, Corvallis, OR, USA.* **Jonathan D. Nash** *is Associate Professor, College of Oceanic and Atmospheric Sciences, Oregon State University, Corvallis, OR, USA.* **Jody M. Klymak** *is Assistant Professor, School of Earth and Ocean Sciences, University of Victoria, Victoria, BC, Canada.*

These unstable profiles are accompanied by high near-bottom turbulence, quantified by the viscous rate of dissipation of turbulent kinetic energy, ε. On average, both density and ε profiles closely resemble those observed during convectively driven mixing in the upper ocean in response to surface cooling or in the lower atmosphere when heated from below. The manner by which this occurs in the bottom Ekman layer is thought to be a result of the combination of the cross-shelf density gradient and the shape of the Ekman velocity profile when the flow atop the bottom layer off Oregon is northward (see Figure 3). As a result of convectively driven near-bottom mixing, the greatest observed values of ε and thickest bottom boundary layers are found during these upwelling relaxation events, providing a clear explanation for the thickened boundary layers previously observed elsewhere under similar conditions (Trowbridge and Lentz, 1991). This process has been implicated in oceanic frontogenesis (Thomas and Lee, 2005) and in the formation of slippery bottom boundary layers predicted from laboratory and numerical experiments (MacCready and Rhines, 1993).

NONLINEAR INTERNAL WAVES

One clearly visible small-scale process in coastal oceans is revealed through long (tens of kilometers) streaks on the sea surface. These streaks are often associated with nonlinear internal waves, sometimes referred to as solitary waves (even though they are rarely solitary), or solitons. They are visible from air and space, although it is the compilations from satellite synthetic aperture radar observations that provide the best evidence for their constant presence in coastal oceans (http://internalwaveatlas.com/Atlas2_index.html). Although these streaks are referred to as waves, part of their highly nonlinear nature may make them more like vortices, in the sense that fluid may be trapped internally as the waves propagate, thereby transporting fluid across the continental shelf (Lamb,

2002; Klymak and Moum, 2003). The leading edges of these waves represent convergence zones, where the ocean surface is ruffled (providing the visible signature) and fluid is displaced downward (providing a supply of near-surface material to subsurface predators). The local food chain can be extensive and active, marked by tuna swarms and dolphins hunting along the wave fronts, a phenomenon long known by local fishermen. Less well known are the biological responses that are internal and rapid, as can be seen in space/time series of acoustics (Figure 4).

Only recently have measurements of the internal structure of the waves been of sufficient fidelity to quantify fundamental aspects of their dynamics. One means of measuring the wave structure uses high-frequency acoustics as an

imaging tool (Farmer and Smith, 1980). The passage of the waves causes deformation of preexisting scattering layers, and under the right conditions, the wave itself can create scattering layers through internal instabilities that create small-scale density microstructure and sound-speed fluctuations. Figure 1 is a dramatic example of this phenomenon. In this image, numerous individual scatterers are evident, likely small fish or zooplankton, as well as coherent scattering layers that describe the outline of the wave and that are thought to be created by small-scale internal deformation within the wave (as in the upper panels of Figure 5; Moum et al., 2003).

Shallow pycnoclines are present in spring and summer off the Oregon coast (Figure 5). They act as waveguides along which waves of depression propagate,
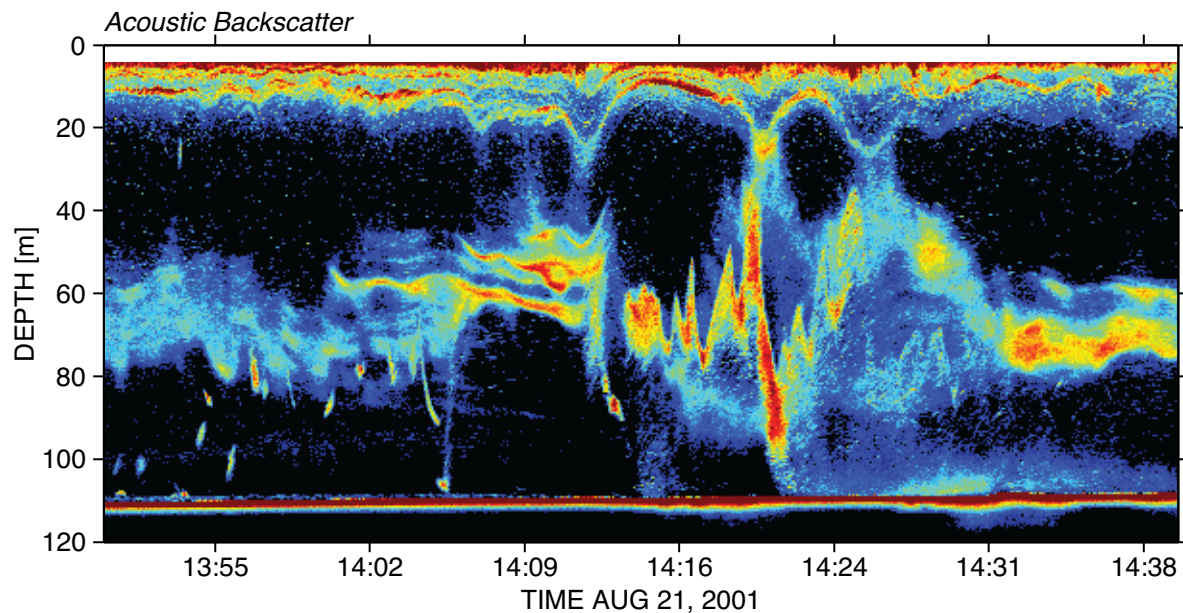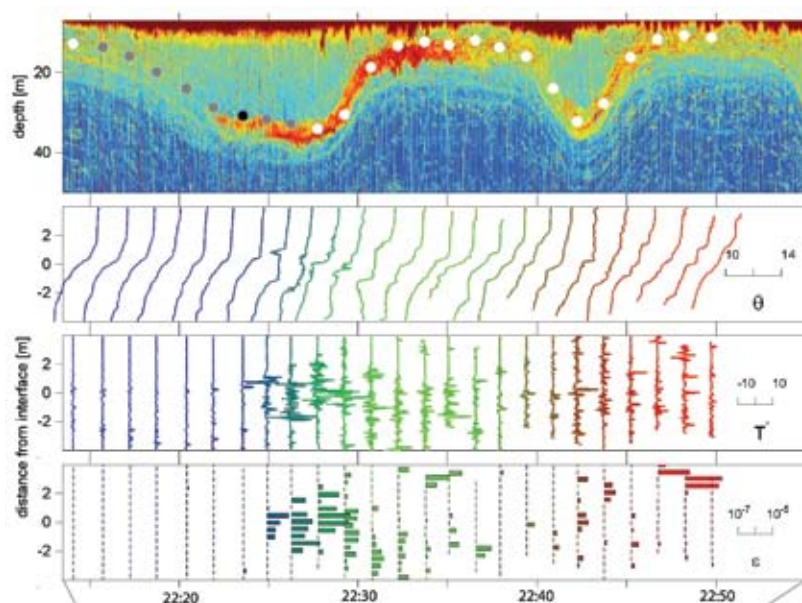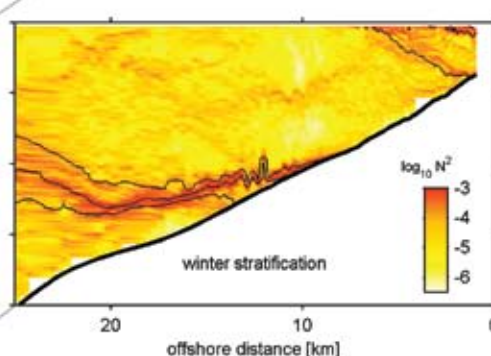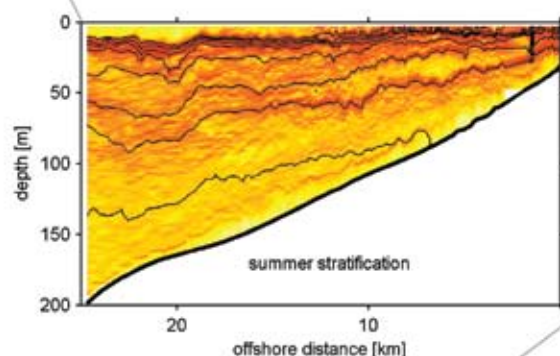

Figure 4. Biological reaction to passing solitary waves on the Oregon Shelf. The image was constructed from hull-mounted acoustic backscatter measurements (120 kHz) over Hecate Bank. The seafloor is seen as a hard (red) target at 112-m depth. Near-surface scattering (likely from zooplankton) shows the passage of a sequence of nonlinear internal waves of depression that propagate along a near-surface thermocline, the first at about 14:12. Prior to the passage of the first wave, there is a relatively horizontal scattering horizon at 60-m depth. Following this, the layer appears to oscillate vertically, moving upward to meet the second wave at 14:20. If we can consider this layer as a contiguous assemblage of zooplankton or small fish, they appear to have swum upward across isopycnals (not shown here) very rapidly (tens of cm s^{-1}) through the phase of the wave with downward vertical velocities. This example is typical of many showing upward motion of deep scattering layers apparently triggered by the passage of nonlinear internal waves.
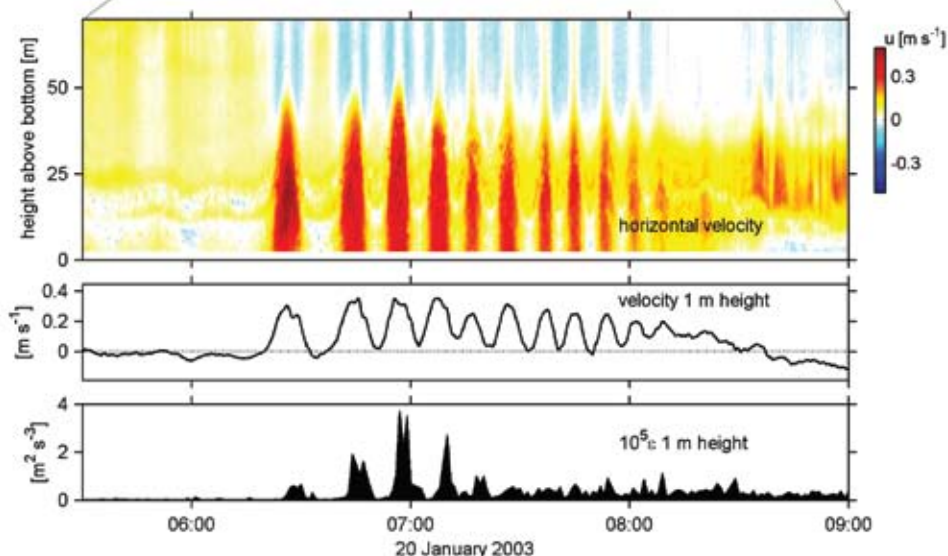
Figure 5. Seasonal differences in nonlinear internal waves. Summertime stratification over Oregon's continental shelf provides a near-surface waveguide that supports waves of depression, examples of which are shown in the uppermost panel. Many of the waves' properties can be measured from ship. High-frequency acoustics helps visualize the waves' structure. The dots represent times at which vertical profiles of density and turbulence were obtained through an isopycnal. The temperature structure immediately above and below that isopycnal is indicated in the second panel, beneath which are shown the temperature fluctuations and high values of the turbulence kinetic energy dissipation rate (ϵ) due to the passage of the waves. In contrast, wintertime stratification provides a near-bottom waveguide that supports waves of elevation. Although these waves can also be measured from ship, they are perhaps best observed from sensors mounted on the seafloor. The lower panels show records from an upward-looking acoustic Doppler current profiler and an acoustic Doppler velocimeter, both mounted at 1-m height above the bottom. Horizontal velocity is in the direction of wave propagation (roughly onshore). The velocity at 1-m height is derived from the velocimeter measurements and the turbulence dissipation at 1-m height by scaling velocity spectra in the inertial subrange. *Adapted from Moum et al., 2003; Moum et al. 2007*

their surface signatures made visible by the patterns of alternating, near-surface fluid convergence/divergence. In winter, near-surface stratification is typically weak and unable to support waves of depression. Instead, near-bottom thermoclines permit the propagation of near-bottom waves of elevation. Although these waves might exhibit a surface signature in shallow water, it is comparatively weak and rarely seen (Zhao et al., 2003). These waves are best sampled from below, where stationary, bottom-mounted landers with rapidly sampled acoustic Doppler current

VARICOSE WAVES

By Emily Shroyer

Nonlinear internal waves of depression and elevation are often seen in the coastal ocean. The terms depression/elevation imply waves that have a mode-1 structure (i.e., all isopycnals are displaced in the same direction, either down or up). Higher-mode waves also exist. Here, we see an example of a wave with mode-2 structure (A) propagating onshore (to the right) followed by a train of short, mode-1 depression waves (B). In the mode-2 wave, isopycnals near the surface are displaced upwards while those at depth are displaced downwards. These waves are sometimes referred to as "varicose" to emphasize the "bulging" nature of the isopycnals. In the middle panel, the background velocity has been removed, leaving the velocity field attributed to the wave. Note the onshore (red) pulse centered at approximately 12 m and the offshore (blue) return flow near the surface. Any return flow beneath the onshore pulse is weak and undetectable in our measurements. Although varicose waves are not as energetic as larger depression waves observed in the same region, they potentially play a significant role in mixing shelf waters. These observations show elevated turbulent kinetic energy dissipation rates (approaching 10^{-4} m^2 s^{-3}) at the trailing edge of the mode-2 wave. Considering the location of these waves in the middle of the pycnocline, this intense mixing may play an important role in eroding the barrier established by the pycnocline, thereby enhancing vertical fluxes of nutrients and heat in the water column.

Emily Shroyer (*eshroyer@coas.oregonstate.edu*) is PhD Candidate, College of Oceanic and Atmospheric Sciences, Oregon State University, Corvallis, OR, USA.
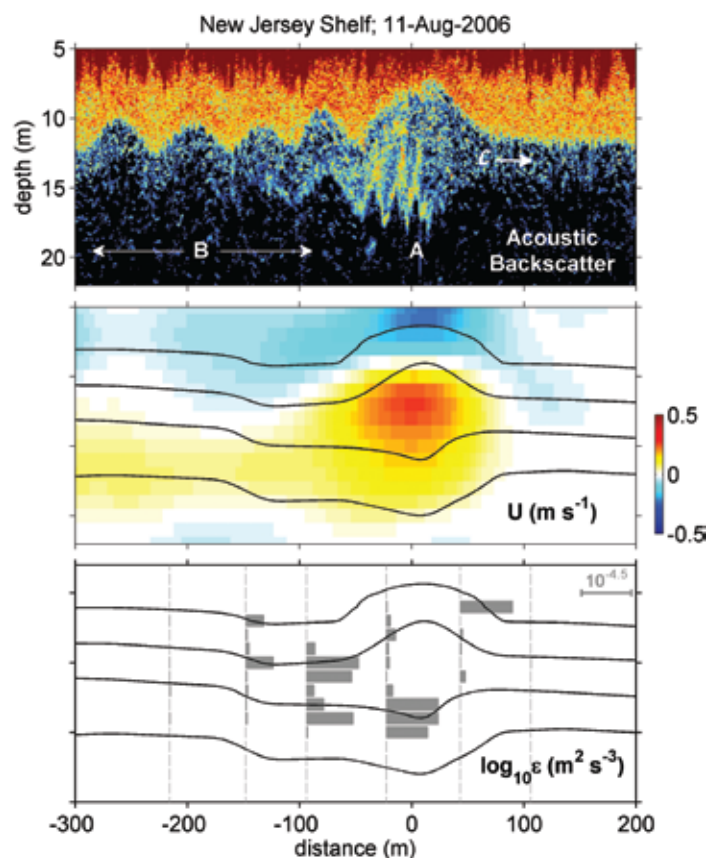
Figure B1. Upper panel: Acoustic backscatter. Middle panel: Onshore wave velocity, U, with isopycnals contoured. Lower panel: Turbulence dissipation rate, from shipboard measurements over the New Jersey shelf in 85-m water depth. Shoreward direction is to the right.

profilers (ADCPs) can provide continuous, high-resolution measurements over long time periods. An example is seen in the lower few panels of Figure 5, where the leading three waves have amplitudes of 30 m. Within each of these waves, near-bottom ε is considerably larger than ambient—either turbulence is explosively generated within the waves or it is being advected along with the wave. The distinction is a matter of some importance. If turbulence is advected by the waves, then fluid must be trapped in the waves and advected with them like a turbulent bore on a beach. This trapped fluid would include the resuspended sediment load created by the large bottom stresses as the waves pass over the bottom (which can be measured optically by profilers—as in Figure 2). Evidence for trapped cores has come from observations that may indicate zooplankton or small fish clouds wholly contained within the leading wave of a near-bottom wave train propagating up the shelf (Klymak and Moum, 2003). Any onshore advection of fluid by elevation waves during periods of coastal downwelling counters the prevailing bottom Ekman transport; it is possible that this is an efficient means of intermittently injecting near-bottom fluid from offshore onto the shelf.

An outstanding question is how nonlinear internal waves are formed. One mechanism, reported by Nash and Moum (2005), shows wave fission from the decelerating, buoyant Columbia River plume. However, this process is local to the plume, and yet these waves are ubiquitous on the shelf. We suspect that nonlinear steepening of internal tides generated at shelf breaks (Holloway et al., 1997) is primarily responsible for

nonlinear wave fields on continental shelves. Although this would seem to be an easily tested mechanism, wave arrivals at a fixed observation point are rarely regular, probably because variations in mesoscale stratification and currents on the shelf alter not only generation locations and timing, but wave propagation as well. The finding that these waves can be simply detected by seafloor pressure measurement (Moum and Nash, 2008) provides some hope for inexpensive, long-term monitoring to assess wave prevalence over continental shelves.

FORM DRAG

One aspect of coastal flows that distinguishes them from those in the main oceanic gyres is their proximity to the bottom. In this sense, coastal flows feel the bottom in a manner similar to the way that atmospheric circulation does: when atmospheric circulation encounters a particularly large obstacle (such as a

mountain range), circulation may be blocked—the flow is diverted either over or around the obstacle. Consequences in coastal flows include accelerated near-bottom velocities (causing enhanced bottom stress) and a pressure drop across the obstacle, resulting in form drag. The exact response is determined by the topographic geometry, local stratification, and flow speed. An unambiguous example of an observed blocked flow over a small bank on Oregon's continental shelf shows some of the main features (Figure 6; Nash and Moum, 2001). The drag exerted by this 2-km feature exerts the equivalent of O(50 km) of flat-bottom stress. Such clear measurement of these flows requires intensive shipboard profiling efforts and, at present, there exist only anecdotes. To determine the net effect of these flows on coastal circulation requires longer-term measurements combined with modeling. One way to do this is by directly measuring
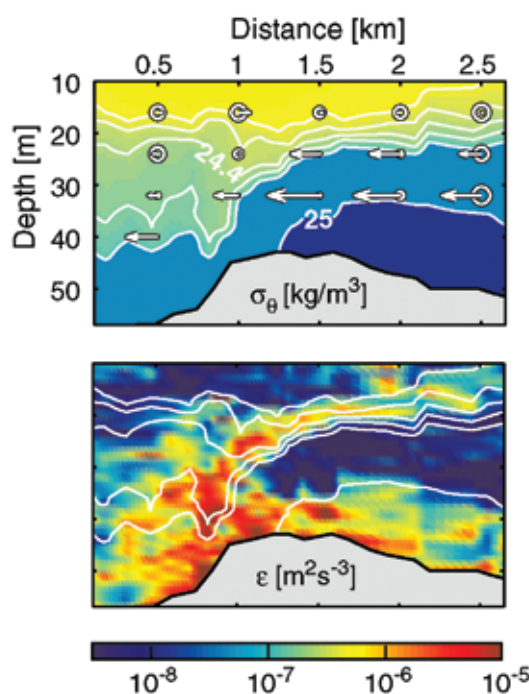

Figure 6. High-drag flow over a topographic obstruction in the coastal ocean. The figure shows the structure of density and ε over Stonewall Bank, a small rise on Oregon's continental shelf. The asymmetry in density structure indicates flow controlled by internal hydraulics, here characterized by a near-bottom flow that is accelerated across the bank from right to left, causing high ε in both the bottom boundary layer and the sheared layer above. The near-bottom flow terminates downstream in a turbulent hydraulic jump. This flow exerts high drag on the overlying flow in the form of intense bottom stresses (skin friction) as well as a net pressure drop (form drag) across the bank. *Adapted from Nash and Moum, 2001*

the pressure drop across the bank with high-resolution seafloor pressure sensors, an effort now underway.

As a consequence of form drag, momentum is extracted from the mean flow—vfrom both the pressure drop across the obstacle and the enhanced bottom stress. Upstream flow blocking and the release of downstream lee waves during unsteady flows can produce nonlocal consequences and stresses, as the resultant radiated waves can transport momentum elsewhere. In the lower atmosphere, where a considerable fraction of the momentum is lost to mountain drag, an accounting of this wave radiation through parameterization is an important part of global circulation models. It is not yet clear how best to reconcile the analogous processes in coastal flows, because we do not know the partitioning of local and remote momentum sinks. Atmospheric waves propagate vertically and break at critical layers in the mesosphere, where they deposit their momentum. However, the free surface of the ocean acts as a reflector, and we do not yet understand how momentum is removed via wave radiation from features like Stonewall Bank or where it is deposited.

THE ROLE OF INTERNAL WAVES IN SHEAR-ENHANCEMENT OF THE COASTAL JET

Away from surface and bottom boundary layers, interior turbulence is strongly linked to the structure of the upwelling-induced coastal jet, and especially to locations where the jet shear is large (Figure 2). Yet, the thermal wind shear alone is of insufficient intensity to trigger shear instability. Continental shelves have a broad spectrum of internal waves, with peaks at near-inertial and tidal periods (Levine, 2002; MacKinnon and Gregg, 2003b; Avicola et al., 2007); the shear associated with this internal wave field is also not typically large enough to trigger shear instability on its own. However, enhanced turbulence is observed where the superposition of thermal wind shear and internal gravity wave shear reduces gradient Richardson numbers to values that are favorable to instability (Figure 7; Avicola et al., 2007). Because the coastal jet is in geostrophic balance to first order, inclusion of a coastal internal wave field is not necessary for a first-order accounting of the coastal circulation. However, the lack of shear in the interior of the geostrophic flow means that it cannot reasonably predict large mixing (or large ε). The internal wave field must also be captured, or at least parameterized. It is possible that jet-wave interactions are not simply linear, so a simple superposition of constituent shear is a naïve approach to assessing potential for instability. The prospects for nonlinear interactions between the coastal
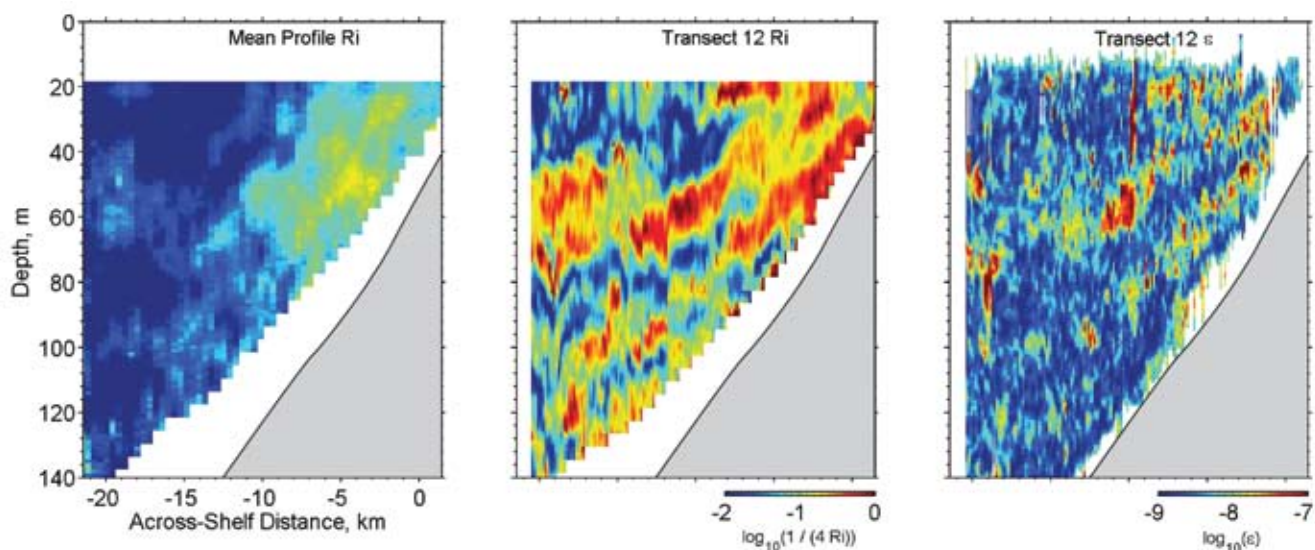

Figure 7. Thermal wind Richardson number (*Ri*) compared to observed *Ri* and ε, each computed from data corresponding to the cross-shelf transect marked +197 h in Figure 2. The left panel shows inverse *Ri* computed using thermal wind shear alone, the middle panel inverse *Ri* computed from the observed shear (4-m scale) and the right panel the observed ε. The critical component of the observed shear is that due to internal waves. Clearly, the thermal wind shear does not display the structure that is observed in the turbulence, ε. *Adapted from Avicola et al., 2007*

TURBULENCE IN RIVER PLUMES

By Levi Kilcher

Shear, stratification, and turbulence associated with tidally driven river plumes far exceed that associated with typical coastal flows, except perhaps during major storms. Acoustic images along an east-west transect across the Columbia River plume reveal the complex structure typical of each tidally pulsed plume. On the ebb of each tidal cycle, a pulse of low-salinity water is released from the river mouth, which in this case detaches from the bottom about 8 km from the river's mouth. Out to about 11.5 km, the near-surface flow thins from 20- to 10-m thickness, is continuously stratified, and has relatively uniform shear and acoustic backscatter. At that point, it transitions: shear, stratification, and turbulence become concentrated at the base of the surface layer (visible in both acoustic backscatter and S^2). Farther offshore, the plume continues to thin, culminating in a 20-m-deep depression at the plume front, which propagates westward at approximately 1 m s^{-1}. Energy dissipation rates within the turbulent head can exceed 10^{-3} m^2 s^{-3}, considerably greater than that within dissipating nonlinear internal waves in the coastal ocean (Moum et al., 2003). The plume front is also a region of strong horizontal velocity convergence, trapping buoyant particles, steepening local surface waves, and potentially enhancing biological productivity. As the plume front decelerates, it can release large-amplitude internal waves (Nash and Moum, 2005), which may propagate 50 km offshore, further extending the influence of the river plume.
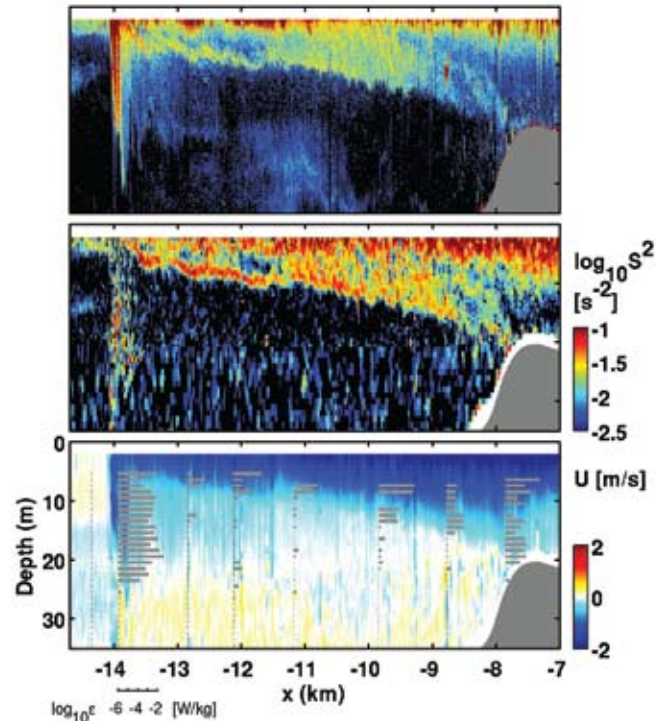

Figure B2. Acoustic backscatter (upper panel), shear squared (middle), and along-axis velocity (lower) within the tidally pulsed plume of the Columbia River in August 2005. Grey bars in the bottom panel show turbulence dissipation rate (scale below). Distances are referenced to the river's mouth to the east.

Levi Kilcher *(lkiltcher@coas.oregonstate.edu) is PhD Candidate, College of Oceanic and Atmospheric Sciences, Oregon State University, Corvallis, OR, USA.*

jet and internal gravity waves have yet to be investigated.

Significantly, because the vertical redistribution of scalars such as heat, biomass, and nutrients is caused by shear-driven mixing associated with the superposition of coastal jet and internal waves, these transports will be underestimated if the turbulence parameterization is based on the subtidal flow alone.

CONSEQUENCES

Detailed observations of coastal processes reveal an impressive variety of phenomena. Although it is clear that these phenomena are all at least locally

important, their role in shaping the character of the low-frequency flow remains an open question. In fact, these observations are, to a large degree, anecdotal. Without a better idea of their prevalence, it will be impossible to determine their importance. Extended, targeted observations will be needed to assess their ubiquity and the prospects for incorporating their dynamics into large-scale models. But, with some knowledge of their properties and of recent numerical experiments, maybe we can identify a couple of significant departures of model from observation.

Low-resolution, low-frequency models do not resolve form drag, nor do they develop sufficient shear to generate the turbulence observed in the interior of coastal upwelling systems. And non-assimilative coastal models can overestimate flow speeds. Could these symptoms result from neglect of the effects of small-scale processes?

The role of the internal wave field may be indicated by comparing the turbulence dissipation rate (ε) as observed at +0 h in Figure 2 to that calculated through a turbulence model embedded in the Princeton Ocean Model (POM), used to compute turbulence fluxes over the same time period (Figure 8; Kurapov et al., 2005b). The model clearly develops turbulence in surface and bottom boundary layers, although the structure (i.e., boundary layer location and thickness) differs from the observations. But perhaps more importantly, the interior is devoid of turbulence, possibly because the model does not contain an energetic internal wave field (high-resolution, two-dimensional model studies by Federiuk and Allen [1996] have produced interior turbulence caused by inertial wave shear via turbulence parameterization). Because the high observed turbulence levels at 30- to 50-m depth inshore of 10 km are in fact coincident with large velocity gradients at the base of the jet, models that lack an internal wave field and associated turbulence may fail to reproduce the correct structure and/or transport of the coastal jet.

The possible importance of form drag is suggested by a different numerical experiment. The correction term in data-assimilative models applied off Oregon opposes the direction of the mean flow, in a depth-averaged sense (Figure 9; Kurapov et al., 2005a). In this case, the required correction is largest in regions of shallow and rough topography, and is of the same order of magnitude as the computed bottom stress. While it is often argued that the correction may be associated with a missing large-scale pressure gradient, the spatial structure of the correction appears linked to the topography. If the missing physics here is form drag, and if it can be properly parameterized numerically, perhaps a significant part of the correction term can be eliminated and the accuracy of forward models increased without data assimilation. Parameterizing and incorporating these processes into the next generation of coastal models ought to be of high priority but will require both significant ingenuity and further extended, detailed measurements as well as enhanced collaborations between observationalists and modelers.

ACKNOWLEDGEMENTS

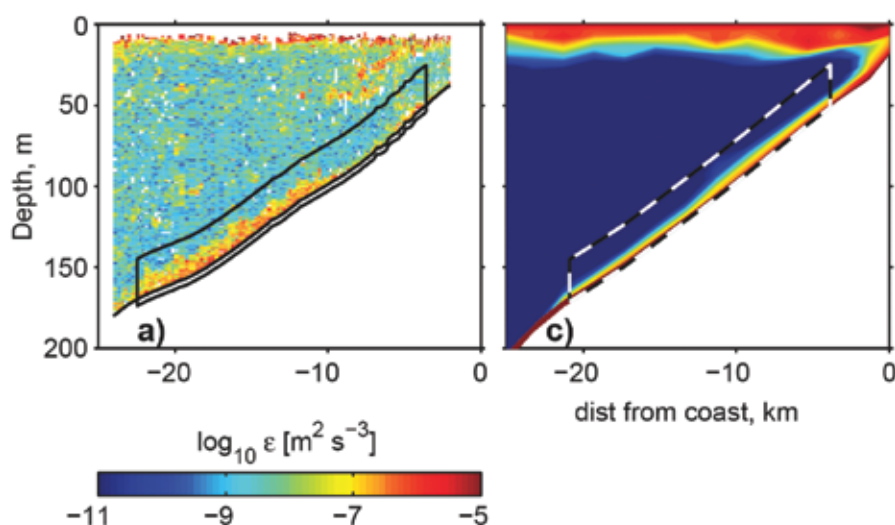Figure 8. Comparison of observed (a) and modeled (c) turbulence dissipation rate (ε) across the Oregon shelf corresponding to the +0 h transect in Figure 2. The model-derived ε incorporates data assimilation of mean flow variables, but the model does not include the tides. *Extracted from Kurapov et al., 2005b*
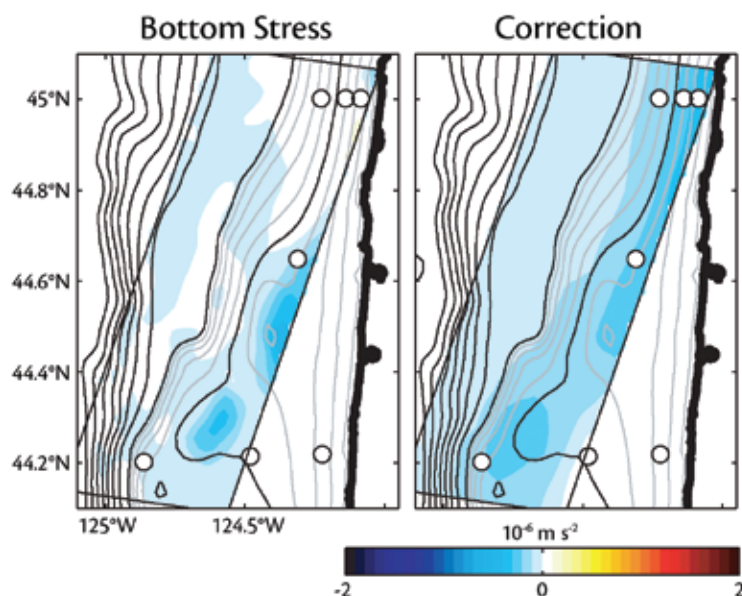
Figure 9. The alongshore momentum correction term required in data-assimilation models is of the same sign and magnitude as the bottom stress, suggesting that an additional momentum sink is not incorporated. This figure shows a comparison of modeled bottom stress (left) and the required correction term (right) in the Oregon shelf depth-averaged momentum budget; black lines are isobaths. Because the correction is highest in regions of shallow water and rough topography, we suggest that missing small-scale physics (in particular, form drag) may be responsible for the required correction. *Extracted from Kurapov et al., 2005a*

in understanding the physical nature of these small-scale flows and how they may contribute to the larger coastal circulation. We are, as always, indebted to the outstanding technical support staff of the Ocean Mixing Group at Oregon State University. Jane Huyer and John Allen contributed helpful comments. ☑

REFERENCES

Avicola, G., J.N. Moum, A. Perlin, and M.D. Levine. 2007. Enhanced turbulence due to the superposition of internal gravity wave shear on the coastal upwelling jet. *Journal of Geophysical Research* 112(C06024), doi:10.1029/2006JC003831.

Farmer, D.M., and J.D. Smith. 1980. Tidal interaction of stratified flow with a sill in Knight Inlet. *Deep-Sea Research* 27:239–245.

Federiuk, J., and J.S. Allen. 1996. Model studies of near-inertial waves in flow over the Oregon continental shelf. *Journal of Physical Oceanography* 26:2,053–2,075.

Holloway, P.E., E. Pelinovsky, T. Talipova, and B. Barnes. 1997. A nonlinear model of internal tide transformation on the Australian North West Shelf. *Journal of Physical Oceanography* 27:871–896.

Klymak, J.M., and J.N. Moum. 2003. Internal solitary waves of elevation advancing on a sloping shelf. *Geophysical Research Letters* 30(20):2,045, doi:10.1029/2003GL017706.

Kurapov, A.L., J.S. Allen, G.D. Egbert, R.N. Miller, P.M. Kosro, M.D. Levine, and T. Boyd. 2005a. Distant effect of assimilation of moored currents into a model of coastal wind-driven circulation off Oregon. *Journal of Geophysical Research* 110(C02022), doi:10.1029/2003JC002195.

Kurapov, A.L., J.S. Allen, G.D. Egbert, R.N. Miller, P.M. Kosro, M.D. Levine, T. Boyd, and J.A. Barth. 2005b. Assimilation of moored velocity data in a model of coastal wind-driven circulation off Oregon: Multivariate capabilities. *Journal of Geophysical Research* 110(C10S08), doi:10.1029/2004JC002493

Lamb, K.G. 2002. Shoaling nonlinear internal waves: On a criterion for the formation of waves with trapped cores. *Journal of Fluid Mechanics* 478:81–100.

Levine, M.D. 2002. A modification of the Garrett–Munk internal wave spectrum. *Journal of Physical Oceanography* 32:3,166–3,181.

MacCready, P., and P.B. Rhines. 1993. Slippery bottom boundary layers on a slope. *Journal of Physical Oceanography* 23:5–22.

MacKinnon, J.A., and M.C. Gregg. 2003a. Mixing on the late-summer New England shelf—Solibores, shear, and stratification. *Journal of Physical Oceanography* 33:1,476–1,492.

MacKinnon, J.A., and M.C. Gregg. 2003b. Shear and baroclinic energy flux on the summer New England shelf. *Journal of Physical Oceanography* 33(7):1,462–1,475.

Moum, J.N., and J.D. Nash. 2008. Seafloor pressure measurements of nonlinear internal waves. *Journal of Physical Oceanography* 38(2):481–491, doi:10.1175/2007JPO3736.1.

Moum, J.N., J.M. Klymak, J.D. Nash, A. Perlin, and W.D. Smyth. 2007a. Energy transport by nonlinear internal waves. *Journal of Physical Oceanography* 37(7):1,968–1,988.

Moum, J.N., A. Perlin, J.M. Klymak, M.D. Levine, T. Boyd, and P.M. Kosro. 2004. Convectively driven mixing in the bottom boundary layer. *Journal of Physical Oceanography* 34:2,189–2,202.

Moum, J.N., D.M. Farmer, W.D. Smyth, L. Armi, and S. Vagle. 2003. Structure and generation of turbulence at interfaces strained by internal solitary waves propagating shoreward over the continental shelf. *Journal of Physical Oceanography* 33:2,093–2,112.

Nash, J.D., and J.N. Moum. 2001. Internal hydraulic flows on the continental shelf: High drag states over a small bank. *Journal of Geophysical Research* 106:4,593–4,611.

Nash, J.D., and J.N. Moum. 2005. River plumes as a source of large-amplitude internal waves in the coastal ocean. *Nature* 437:400–403, doi:10.1038/nature03936

Perlin, A., J. N. Moum, and J.M. Klymak. 2005a. Response of the bottom boundary layer over a sloping shelf to variations in alongshore wind. *Journal of Geophysical Research* 110(C10S09), doi:10.1029/2004JC002500.

Perlin, A., J.N. Moum, J.M. Klymak, M.D. Levine, T. Boyd, and P.M. Kosro. 2005b. A modified law-of-the-wall to describe velocity profiles in the bottom boundary layer. *Journal of Geophysical Research* 110(C10S10), doi:10.1029/2004JC002310.

Simpson, J.H., W.R. Crawford, T.P. Rippeth, A.R. Campbell, and J.V.S. Choek. 1996. The vertical structure of turbulence dissipation in shelf seas. *Journal of Physical Oceanography* 26:1,579–1,590.

Thomas, L.N., and C.M. Lee. 2005. Intensification of ocean fronts by down-front winds. *Journal of Physical Oceanography* 35:1,086–1,102.

Trowbridge, J.H., and S.J. Lentz. 1991. Asymmetric behavior of an oceanic boundary layer over a sloping bottom. *Journal of Physical Oceanography* 21:1,171–1,185.

Zhao, Z., V. Klemas, Q. Zheng, and X. Yan. 2003. Satellite observations of internal solitary waves converting polarity. *Geophysical Research Letters* 30, doi:10.1029/2003GL108286.